Human Reproduction, Vol.25, No.9 pp. 2188–2202, 2010
Advanced Access publication on July 3, 2010 doi:10.1093/humrep/deq168

human reproduction

ORIGINAL ARTICLE *Andrology*

Expression of a truncated form of KIT tyrosine kinase in human spermatozoa correlates with sperm DNA integrity

Barbara Muciaccia[1], Claudio Sette[2], Maria Paola Paronetto[2], Marco Barchi[2], Simona Pensini[1], Angela D'Agostino[1], Loredana Gandini[3], Raffaele Geremia[2], Mario Stefanini[1], and Pellegrino Rossi[2,*]

[1]Department of Histology and Medical Embryology, University of Rome 'La Sapienza', Rome, Italy [2]Department of Public Health and Cell Biology, Facolta' di Medicina e Chirurgia, University of Rome 'Tor Vergata', via Montpellier 1, Rome 00133, Italy [3]Seminology Laboratory - Sperm Bank of the Department of Medical Physiopathology, University of Rome 'La Sapienza', Rome, Italy

*Correspondence address. Tel: +39-06-72596272; Fax: +39-06-72596268; E-mail: pellegrino.rossi@med.uniroma2.it

Submitted on April 16, 2010; resubmitted on May 27, 2010; accepted on June 4, 2010

BACKGROUND: TR-KIT, a truncated form of KIT (the KITL receptor), corresponding to the c-terminal half of the intracellular split tyrosine kinase domain, is expressed during the haploid stages of mouse spermatogenesis, and is one of the candidate sperm factors possibly involved in egg activation at fertilization.

METHODS: Immunocytochemistry of adult human testis, and studies of human semen samples from volunteer donors through immunofluorescence, confocal microscopy, flow cytometry, western blot and RT–PCR analyses were performed.

RESULTS: We show that the TR-KIT is expressed during spermiogenesis in the human testis, and that it is maintained in human ejaculated spermatozoa. TR-KIT is localized both in the equatorial segment and in the sub-acrosomal region of the human sperm head. The equatorial localization of the TR-KIT persists after the spontaneous acrosome reaction. Cytometric analysis of several sperm samples from volunteer donors, showed variable degrees of the TR-KIT-specific immunolabeling, and a significant inverse correlation (Pearson's coefficient, $r = -0.76$, $P < 0.0001$, $n = 23$) of the TR-KIT positivity with markers of sperm damage, i.e. DNA fragmentation, as revealed by terminal deoxynucleotidyl transferase-mediated deoxyuridine triphosphate-nick end labeling (TUNEL) analysis and the intense clusterin positivity. We also found less significant inverse correlation with altered head morphology ($r = -0.47$, $P < 0.05$, $n = 23$) and direct correlation with sperm forward motility parameters ($r = 0.59$, $P < 0.01$, $n = 23$).

CONCLUSIONS: The TR-KIT is present in the equatorial region of human spermatozoa, which is the first sperm component entering into the oocyte cytoplasm after fusion with the egg. This localization is consistent with the function previously proposed for this protein in mice. In addition, the TR-KIT represents a potential predictive parameter of human sperm quality.

Key words: TR-KIT / human spermatozoa / equatorial segment / DNA damage / clusterin

Introduction

The KIT receptor tyrosine kinase (KITL receptor) plays an essential role in the mitotic stages of mouse spermatogenesis (Sette *et al.*, 2000; Rossi *et al.*, 2000, 2003; Pellegrini *et al.*, 2008), but with the onset of meiosis its expression, at both the RNA and protein level ceases. After meiosis the TR-KIT, a truncated form of KIT corresponding to the c-terminal half of the intracellular split tyrosine kinase domain, is expressed beginning at the round spermatid stage (Sorrentino *et al.*, 1991; Rossi *et al.*, 1992). The mouse TR-KIT is originated by transcription of an alternative mRNA from a cryptic promoter in the 16th intron of the mouse *KIT* gene, which is active during spermiogenesis (Albanesi *et al.*, 1996). TR-KIT localizes to the residual cytoplasm, midpiece and the post-acrosomal region of the mouse epididymal spermatozoa (Albanesi *et al.*, 1996; Sette *et al.*, 1997). Microinjection of the recombinant TR-KIT into metaphase II-arrested mouse oocytes triggers events of early embryogenesis, such as cortical granule exocytosis, completion of the second meiotic division, formation of pronuclei, and development up to the morula stage (Sette *et al.*, 1997). The TR-KIT-mediated parthenogenetic egg activation

requires its interaction with Fyn (a Src-like kinase) and the adaptor protein Sam68, with the consequent activation of phospholipase Cγ1 within the egg cytoplasm (Sette *et al.*, 1998, 2002; Paronetto *et al.*, 2003). Interestingly, Fyn and/or other egg-carried Src-like kinases have been shown to play a critical role in egg resumption from meiosis II at fertilization and the subsequent zygotic development in mammals (Meng *et al.*, 2006; McGinnis *et al.*, 2007; Reut *et al.*, 2007; Tomashov-Matar *et al.*, 2008; Luo *et al.*, 2009; Levi and Shalgi, 2010).

Thus, the TR-KIT has been proposed as a sperm factor possibly involved in sperm-mediated egg activation at fertilization (Rossi *et al.*, 2003). However, it cannot be excluded that the TR-KIT, besides its eventual participation to the egg activation process at fertilization, plays additional roles during mouse spermatogenesis or in the mature sperm cell function.

Restricted expression of KIT in the membrane of spermatogonia and of TR-KIT in the cytoplasm of spermatids was also observed in the rat seminiferous epithelium, both at the RNA and protein level (Prabhu *et al.*, 2006). As in rodents, in the adult human testis full-length KIT is expressed in spermatogonia, as revealed by the use of antibodies directed against the KIT extracellular domain (Natali *et al.*, 1992; Strohmeyer *et al.*, 1995; Sandlow *et al.*, 1996). However, no clear information is available about the possible expression of TR-KIT in post-meiotic stages in human testis. Immunocytochemical analysis using a polyclonal antibody directed against the human KIT c-terminus (Santa Cruz, C-19, cat. no. sc-168), which recognizes both full-length KIT and TR-KIT, showed positivity in spermatogonia and in elongating spermatids of marmoset monkeys, but not in meiotic spermatocytes, similarly to reported observations in rodents (von Schonfeldt, 1999). Using the same antibody, Feng *et al.* (2005) reported immunocytochemical reactivity at the level of the acrosome in the human sperm head, but, on the basis of western blot analysis, they claimed that this positivity was due to the 150 kDa full-length KIT. In a recent study, using another antibody directed against the human KIT c-terminus (Dako, Anti-Human CD117, cat. no. A4502), KIT positivity within the human testis was confined to spermatogonia and spermatids, whereas no staining was found in meiotic spermatocytes, nor in Sertoli cells, suggesting a pattern of expression of the two alternative products of the *KIT* gene analogous to that observed in rodents (Unni *et al.*, 2009). Even more recently, by using a further polyclonal antibody directed against the c-terminus of human KIT (Abcam, cat. no. ab16832), KIT immunoreactivity in human spermatids was also evident (He *et al.*, 2010).

A truncated form of KIT analogous to mouse TR-KIT is aberrantly expressed in human cancer cell lines of various origin and in primary prostate malignant tumors both at the RNA and protein level (Toyota *et al.*, 1994; Takaoka *et al.*, 1997; Paronetto *et al.*, 2004). The aberrant transcript encoding human TR-KIT originates from a cryptic promoter present within the 15th intron of the human *KIT* gene (Toyota *et al.*, 1994; Paronetto *et al.*, 2004), and not from the 16th intron, which appears to be the functional TR-KIT promoter only in mice (Sakamoto *et al.*, 2004). Interestingly, murine hematopoietic stem cells and multipotent progenitors express the TR-KIT at the RNA and protein level, so that a potential role for this protein in the self-renewal of these cells has been postulated (Zayas *et al.*, 2008). The TR-KIT ability to activate early embryonic development when microinjected into mouse eggs, its expression in hematopoietic stem cells, and its aberrant expression in human tumors, in which it activates Src-like kinase activity (Paronetto *et al.*, 2004), suggest an important role of these intracellular alternative *KIT* gene products in regulating developmental events involving growth factor-independent cell proliferation.

Among assisted reproduction techniques (ART), the intracytoplasmic sperm injection (ICSI) is overall considered a 'safe' technique, however, it bypasses the natural mechanisms of gamete selection. In particular, the injection of spermatozoa-carrying DNA damage might be dangerous in terms of potential malformations in the conceived child (Lewis, 2002). Moreover, DNA damage in the male germ line, mostly due to oxidative stress (Agarwal *et al.*, 2008), has been associated with male infertility, failed fertilization, impaired preimplantation development and poor pregnancy outcomes, whether the insemination is natural or artificial (Irvine *et al.*, 2000; Agarwal and Said, 2003; Aitken *et al.*, 2009; Barratt *et al.*, 2010). A significant increase in DNA damage can also be found in sperm from infertile men classified as normozoospermic on the basis of normal standard sperm parameters (Saleh *et al.*, 2002). Thus, discovery of new sperm parameters predictive of DNA integrity will have an important impact on the development of ARTs.

In the present paper, we have investigated the expression of the TR-KIT in human ejaculated spermatozoa from the seminal fluids of volunteer donors. We found that TR-KIT, but not full-length KIT, is present in the equatorial and sub-acrosomal region of the human sperm head. Moreover, our results show a significant positive correlation of the TR-KIT positivity with sperm DNA integrity, and we therefore propose the TR-KIT as a new potential marker of human semen quality.

Materials and Methods

Semen samples

Specimens from 23 reputedly normozoospermic volunteer donors attending the Seminology Laboratory - Sperm Bank of the Department of Medical Physiopathology, University of Rome 'La Sapienza', were collected by masturbation after 3–5 days of sexual abstinence, into sterile plastic jars. Material was utilized after having obtained written a consent for the utilization of semen samples. Samples were allowed to liquefy for 60 min at 37° C and were then evaluated according to WHO criteria (World Health Organization, 1999). The variables taken into consideration were: ejaculate volume (ml), sperm concentration ($n \times 10^6$/ml), total sperm count ($n \times 10^6$/ejaculate), forward motility (%) and morphology (% abnormal forms). None of the donors were found to be oligospermic. Of the 23 donors, 20 were within the normal standard parameters defined by WHO (normozoospermic), whereas the remaining 3 were borderline asthenoteratozoospermic. After removing seminal plasma by centrifugation, sperm pellets were washed twice in 1× phosphate-buffered saline (PBS), counted and divided into aliquots.

For swim-up purification of semen samples, 1 μl of each seminal sample was diluted 1:2 with Hank's medium and centrifuged for 10 min at 300 g. After centrifugation, the supernatant was discarded and an aliquot of 0.5 ml of Hank's was layered on the pellet. The spermatozoa were allowed to migrate for 30 min at 37°C. After migration, the supernatant was gently aspirated and processed for further studies.

Immunohistochemistry and immunocytochemistry

Histological sections from two formalin-fixed paraffin-embedded human testicular normal tissue fragments obtained from orchiectomy of testicular cancer patients (a gift from Dr Giovanni Bertalot, Ospedale di Leno, Brescia, Italy) were cut into 5-μm sections and mounted on polylysine coated slides. Sections were dewaxed, rehydrated and processed in a microwave for antigen retrieval in pH 6.0 citrate buffer. After quenching of endogenous peroxidase and blocking of non-specific binding, sections were incubated for 1 h at room temperature (RT) with 1:200 polyclonal antibody directed against the human KIT c-terminus (Santa Cruz, C-19, cat. no. sc-168), which recognizes both full-length KIT and TR-KIT, extensively washed and then processed using the avidin–biotin peroxidase complex (ABC) procedure, according to the manufacturer's protocol (UltraTek HRP Anti-Polyvalent kit, ScyTek Laboratories, USA), negative controls were performed using affinity-purified rabbit IgG or omitting the primary antibody. Peroxidase activity was revealed using 3,3-diaminobenzidine tetrahydrochloride (Roche, Italy), nuclei were quickly counterstained with Mayer's hematoxylin. After washing, sections were permanently mounted and observed by light microscopy.

For immunocytochemical studies on human semen samples, we used the same UltraTek HRP Anti-Polyvalent kit and protocol described above. In particular before primary antibody incubation, ejaculated spermatozoa, obtained after washing of sperm pellets and spotted into polylysine coated slides, were briefly treated with cold acetone (to fix and simultaneously permeabilize cells) and air dried. Samples were mounted on slides and observed by light and phase-contrast microscopy. No staining was evident with non-immune rabbit IgG, nor with the secondary antibody alone. No nuclear counterstaining was performed.

Immunofluorescence analysis and confocal microscopy

Ejaculated spermatozoa, obtained after sperm pellet washing, were spotted into polylysine coated slides, fixed in cold acetone and air dried. After blocking for 2 h at RT with 1× PBS/5% bovine serum albumin (BSA 5%)/ normal goat serum (NGS) 10% [or 10% NGS plus 10% normal donkey serum (NDS) in double-immunostaining experiments], sperm cells were incubated overnight (O/N) at 4°C with 1:200 C-19 rabbit anti-human KIT antibody, extensively washed, incubated for 1 h at RT with 1:1000 secondary goat anti-rabbit Alexafluor 488-conjugated antibody (Molecular Probes), washed, mounted and observed at fluorescence microscopy (Axioplan 2 Imaging system, Carl Zeiss, Germany). Negative controls were performed omitting primary antibodies and using the affinity-purified rabbit IgG. Nuclei were stained using TOTO-3 dye (1:2000; Sigma Aldrich, Italy). In order to assess the specificity immunobinding of C-19 polyclonal antibody to the human intracellular KIT sperm antigen, before the immunostaining, primary antibody was preadsorbed with a 100-fold mass excess of the immunogenic cognate peptide (Santa Cruz Biotechnology) and then used in paired control slides to evaluate the efficiency of competition; this experiment was repeated three times on different semen samples.

In order to perform double-immunostaining for the TR-KIT and acrosin, incubation for 1h at RT with 1:500 mouse monoclonal anti-human acrosin antibody (Biosonda Corp., Chile) was performed after O/N C-19 anti KIT incubation, whereas secondary antibodies, 1:1000 secondary Alexafluor 488 goat anti-rabbit (Molecular Probes, Invitrogen) and 1:300 donkey Cy3-conjugated anti-mouse (Jackson ImmunoResearch, UK), were used together for 1h at RT. Nuclei were stained using TOTO3 dyes (1:2000; Molecular Probes, Invitrogen). Labeled-sperm cells were observed with a Leica laser scanning microscope TCS SP2 equipped with three laser lines. Each channel was acquired separately using specific laser lines to avoid a bleed-through of the fluorochromes. Photomicrographs were acquired using LAS AF Leica Confocal Software (Leica, Germany).

Immunoblot analysis

Human spermatozoa from raw semen of normozoospermic donors and from patients recruited for fertility studies were resuspended in lysis buffer (50 mM HEPES, pH7.5, 150 mM NaCl, 15 mM MgCl2, 15 mM EGTA, 250 mM NaVO4, 10 mM b-glycerophosphate, 1% Triton X100, 0.1% SDS, supplemented with protease inhibitor cocktail) and sonicated for three cycles of 30 s on ice. The control recombinant mouse TR-KIT protein was prepared by protein extraction from transfected cell lines as described previously (Albanesi *et al.*, 1996; Sette *et al.*, 1997). Lysates were cleared by centrifugation at 10 000 g for 10 min. The supernatant fraction was collected, diluted in SDS-PAGE sample buffer and boiled for 5 min. Samples were separated on 10% SDS-PAGE gels and transferred to polyvinylidene fluoride Immobilon-P membranes (Millipore) using a semidry blotting apparatus (BioRad). Western analysis was carried out as previously reported (Sette *et al.*, 2002) using the C-19 anti-human KIT (c-terminal) antibody (1:1000 dilution) O/N at 4°C. Competition was performed by preincubating the antibody with an excess of the immunogenic peptide (100 × molar excess; 1:1 mass ratio) for 12 h before dilution in the primary antibody solution for hybridization (Sette *et al.*, 1997). Secondary anti-rabbit IgG conjugated to horseradish peroxidase (Amersham) were incubated with the membranes for 1 h at RT at a 1:10 000 dilution in PBS containing 0.1% Tween 20. Immunostained bands were detected by the chemiluminescent method (Santa Cruz Biotech.). The human semen sample in which 100% of spermatozoa lacked the acrosome was kindly provided by Dr Jan Tesarik (Center for Reproductive Medicine, European Hospital, Rome, Italy).

For the RNA interference analysis in transfected cell lines, a 500-bp inverted repeat corresponding to part of the 5′ untranslated region and the beginning of the mouse TR-KIT open reading frame (ORF) (Rossi *et al.*, 1992) was subcloned in the pDECAP vector described by Shinagawa and Ishii (2003). HEK293 cells were co-transfected with a recombinant plasmid expressing the mouse TR-KIT ORF (Albanesi *et al.*, 1996; Sette *et al.*, 1997) and a second plasmid expressing an Myc epitope (to control for transfection efficiency). Cells were also co-transfected either with the pDECAP empty vector or with increasing amounts of the interfering plasmid constructs. Protein extracts from transfected cells were processed for immunoblot analysis. Western blots were probed with the C-19 anti-human-KIT-c-terminus antibody and an antibody directed against the Myc epitope.

RT–PCR analysis

In order to verify the presence of specific KIT mRNA molecules in sperm cells following osmotic shock, the total RNA was extracted from 2×10^6 purified ejaculated spermatozoa as previously described (Muciaccia *et al.*, 2007) using high pure RNA isolation kit (Roche) according to the manufacturer's instructions. Purified RNA was treated for 15 min at 37°C with 2 units of Deoxyribonuclease I, Amplification Grade (Invitrogen-Life technologies) to prevent DNA genomic contamination. An aliquot of total RNA was reverse-transcribed, using Sensiscript Reverse Transcriptase (Qiagen), a highly sensitive enzyme recommended for very small RNA amount (<50 ng) and oligo-dT as primer. Then, by PCR amplification, total RNA was tested for protamine-2 gene (PRM-2, specifically expressed only in haploid germ cells), using a primer set able to discriminate between genomic DNA and sperm mRNA (Miller *et al.*, 1994).

In order to amplify KIT mRNA and discriminate between different transcripts (full-length mRNA or truncated form), aliquots of cDNA were used in amplification reactions using the following oligonucleotide primers

spanning four contiguous human KIT gene exons (Accession number: nG_007456): e15 (forward) GTACTAATGAGTACATGGACATG; e16 (forward) GCTCATACATAGAAAGAGATGTG; e17 (forward) TGTATT CACAGAGACTTGGCAGC; e18 (reverse) TGCTTTCAGGTGCCAT CCACTTCAC.

Amplification conditions were: first denaturation at 94°C for 3 min, then 94°C for 30 s, 65°C for 45 s, 72°C for 40 s for 50–80 cycles, in 50 μl final volume using 2 U of *Taq* DNA polymerase (Roche). A control reaction tube, in which reverse transcriptase enzyme was omitted, was also included to test possible DNA genomic contamination. Aliquots of PCR product (i.e. 1/5 of total reaction volume) were separated on 2% agarose gel and visualized by ethidium bromide staining.

Cytometric analysis of human sperm cells

Presence of intracellular TR-KIT and clusterin antigens on freshly isolated sperm cells from presumably healthy donors was assessed by cytometric analysis. Aliquots of 10^6 sperm cells/tube were briefly fixed on ice using 2% paraformaldehyde, washed twice and then permeabilized using 0.1% sodium citrate/0.1% Triton X-100. After washing sperm cells were incubated for 30 min on ice with primary antibodies (1:200 in PBS/1% BSA, C-19 rabbit polyclonal antibody against the c-terminus of human KIT, #sc-168; H-330 polyclonal rabbit anti-human clusterin antibody, #sc-8354, both from Santa Cruz Biotechnology, Germany). The C-19 antibody recognizes both the full-length KIT and the TR-KIT, whereas the anti-clusterin antibody can recognize either the acrosomal or the surface isoforms of clusterin. Sperm cells from the same samples were also incubated in a control tube with the same concentration of the corresponding affinity-purified rabbit IgG (Sigma), as recommended by technical data sheets. Antibody-labeled sperm suspensions were washed twice with 1 × PBS/1% BSA, incubated with phycoerythrin-conjugated secondary antibody (Goat anti-rabbit-PE, by Jackson ImmunoResearch Laboratories, UK). In order to assess the presence of intracellular TR-KIT and to exclude its sperm surface expression, control tube reactions were also performed using aliquots of unfixed and unpermeabilized sperm cells in which the anti-KIT antibody immunolabeling failed to detect any surface specific signal (data not shown). The specificity of the sperm cells gate was verified by analysis of sperm DNA content using the DNA binding dye propidium iodine. For double detection of both the TR-KIT antigen and the sperm DNA fragmentation by the terminal deoxynucleotidyl transferase-mediated deoxyuridine triphosphate-nick end labeling (TUNEL) technique, aliquots of 1×10^6 spermatozoa were treated by *In Situ* Cell Death Detection Kit-Fluorescein (Roche, Italy), according to the manufacturer's instructions before the TR-KIT immunolabeling. Cells were then run through a flow cytometer (Epics XL Beckman Coulter, USA) using an Argon 488 nm excitation laser and 5000 and 10 000 events were, respectively, acquired for each single and double reaction/tube. Results were expressed as the percentage of positive spermatozoa gated. In order to assess the specificity immuno-binding of C-19 polyclonal antibody to human intracellular TR-KIT sperm antigen, before cytometric analysis, primary antibody was pre-adsorbed with a 100-fold mass excess of the immunogenic cognate peptide (Santa Cruz Biotechnology) and then used in paired control tubes to evaluate the efficiency of competition binding reaction; the competition experiment was repeated four times on different semen samples.

Statistical analysis

Data from morphological and cytometric analyses of semen samples were utilized to build matrixes for the calculation of *r*-values (Pearson's product-moment correlation coefficients); the significance (two-tailed probability values) of *r* coefficients were calculated on the basis of the correlation values and the sample sizes.

Results

Immunohistochemistry in normal adult testis

Using a polyclonal antibody directed against the c-terminus of human KIT (Santa Cruz, C-19, sc-168), which recognizes both the full-length KIT and the TR-KIT, the KIT immunostaining was evident in the membrane of several spermatogonia in the basal layer and in interstitial Leydig cells, whereas Sertoli cells and spermatocytes inside the seminiferous tubules were negative (Fig. 1A–C). Clear positivity was also evident in the haploid stages of spermatogenesis. KIT immunostaining was evident in the cytoplasm of round (Fig. 1A and B) and elongating spermatids (Fig. 1C), sometimes with a distinct perinuclear distribution in the area of the developing acrosome (Fig. 1B). The presence of KIT immunostaining both in spermatogonia and in spermatids, but not in spermatocytes, is substantially similar to recent observations by other groups using two different polyclonal antibodies directed against the c-terminus of human KIT (Unni *et al.*, 2009; He *et al.*, 2010).

Analysis of ejaculated spermatozoa by immunocytochemistry

Preparations of freshly ejaculated spermatozoa from normozoospermic subjects were fixed after permeabilization and probed with the C-19 anti-human KIT antibody, followed by secondary antibody conjugated to peroxidase (Fig. 1D and E). Immunocytochemical analysis revealed KIT staining in the anterior region of the sperm head, with maximal intensity often observed in the equatorial segment (Fig. 1D), or isolated intense staining in the equatorial segment alone (Fig. 1E). However, not all sperm heads resulted positive to the KIT immunostaining (Fig. 1D). Notably, most of KIT-negative spermatozoa appeared to have mis-shaped heads or other evident anomalies extending to the midpiece (Fig. 1D).

Immunofluorescence and cytometric analysis of ejaculated spermatozoa

A typical low magnification picture of fixed-permeabilized sperm preparation from a normozoospermic patient probed for immunofluorescence with the anti-human KIT antibody (green-cyan signal), and counterstained with TOTO-3 dye to identify sperm nuclei (blue signal), is shown in Fig. 2A. Similar to immunocytochemistry observations, KIT positivity was evident in most sperm heads, especially in the equatorial segment, but, again, not all spermatozoa appeared to be positive. Figure 2B shows that the fluorescent signal was almost completely abolished if the primary antibody had been pre-incubated with a 100-fold mass excess of the immunogenic peptide, demonstrating specificity of KIT immunostaining in the sperm head.

In order to quantify positivity of KIT immunostaining, we performed cytometric analysis. A typical example of fluorescence-activated cell sorting (FACS) analysis with a permeabilized sperm sample from a normozoospermic subject is shown in Fig. 2C. Specificity of the shift (red line) was confirmed by its abolishment after pre-incubation of the primary antibody with the immunogenic peptide (Fig. 2C, blue line). KIT positivity in spermatozoa varied in different subjects, ranging from 10 to 93%, with a median of 54% (Table I). No shift was obtained with the same antibody if sperm samples had not

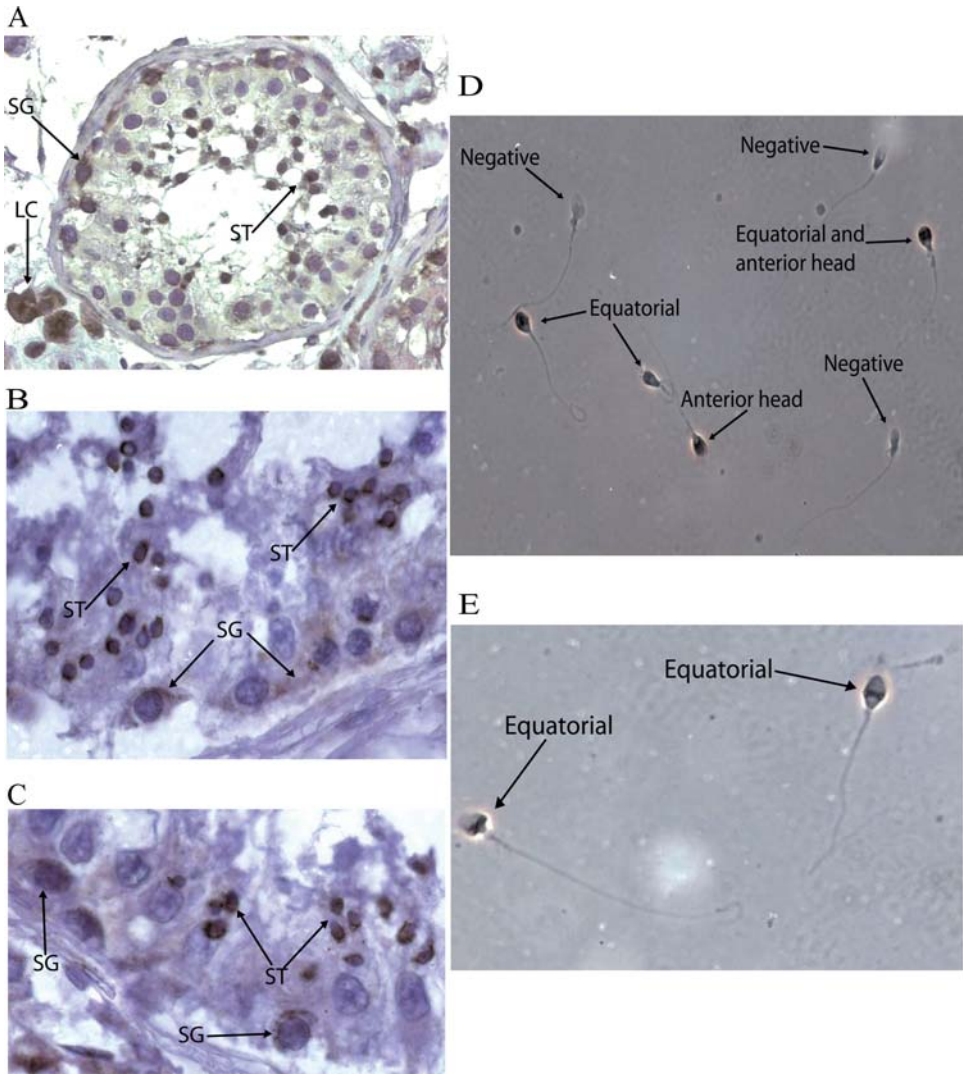

Figure 1 Immunohistochemical and immunocytochemical studies of human testis and spermatozoa with an anti-KIT (c-terminal) antibody. Localization of KIT immunostaining in histological sections of normal adult testis (**A–C**) and in permeabilized spermatozoa from semen of normozoospermic donors (**D** and **E**) using the C-19 rabbit polyclonal antibody against the c-terminus of human KIT. Staining was revealed with a secondary antibody conjugated to peroxydase (hematoxylin counterstained). Light microscope images at lower (A and D) and higher (B, C and E) magnifications are shown. In (D and E), light microscope images were merged with phase contrast pictures. Arrows in (A–C) indicate positive staining in spermatogonia (SG), spermatids (ST) within the seminiferous tubules, and in interstitial Leydig cells (LC). Arrows in (D and E) indicate either absence of staining (negative) or staining in the equatorial and anterior head regions of spermatozoa.

been permeabilized (data not shown), indicating that the KIT positivity is due to intracellular sperm components.

Subcellular localization of KIT immunostaining in human sperm heads

Typical double immunofluorescence analysis performed with anti-KIT (green) and anti-acrosin (red) antibodies, confirmed that the KIT–positivity in human sperm was localized in the anterior region of the head, with maximal intensity in the equatorial segment, behind the acrosome, or exclusively in the equatorial region (Fig. 3A; see also Supplementary Material, Fig. S2A). Notably, KIT equatorial staining persisted in acrosin-negative sperm heads, indicating that it is not localized in the acrosome vesicle nor released during spontaneous acrosome reaction. In some sperm heads, KIT and acrosin signals appeared to uniformly merge all over the anterior region of the head (yellow signal), with no evident accumulation in the equatorial segment. Some sperm heads were KIT-negative, but positive for acrosin staining, or negative for both signals. Careful morphological analysis of KIT positivity in sperm samples from several normozoospermic volunteer donors indicated that 50–80% of KIT-positive spermatozoa showed maximal or isolated staining in the equatorial segment, whereas the remaining percentage of sperm cells showed apparent merging of the KIT and acrosin signals in the anterior region of the head. When DNA counterstaining (blue signal in Fig. 3A) was omitted, it was evident that also in spermatozoa

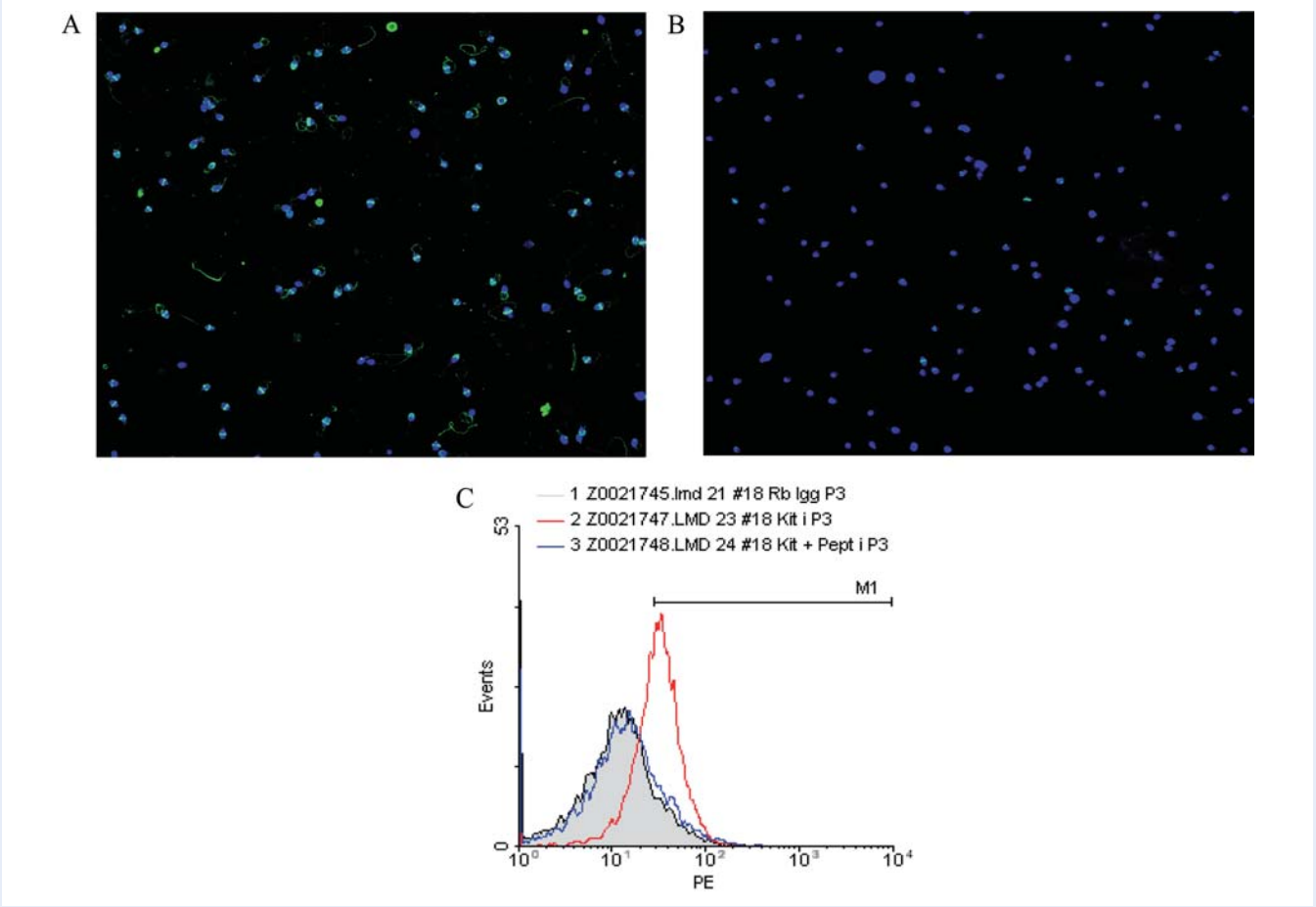

Figure 2 Immunofluorescence and cytometric analysis of permeabilized human spermatozoa with an anti-KIT (c-terminal) antibody. (**A**): immunofluorescence analysis of permeabilized spermatozoa from semen of a normozoospermic donor, using the C-19 rabbit polyclonal antibody against the c-terminus of human KIT (green/cyan signal) and TOTO-3 dye counterstaining of DNA in sperm heads (blue signal). KIT positivity is evident in the equatorial segment of most sperm nuclei. (**B**): same as in (A), except that the C-19 antibody had been previously incubated with an excess of the KIT c-terminal immunogenic peptide. KIT staining is no longer evident in most of the sperm heads. This experiment was repeated with similar results on three different sperm samples. (**C**): representative example of quantification of the percentage of KIT positivity in permeabilized human sperm samples using flow cytometry with the C-19 antibody. Specificity of the shift (red line) was confirmed by its abolishment after pre-incubation of the primary antibody with the immunogenic peptide (blue line, which coincides with the black line obtained with non-immune IgGs). This experiment was repeated with similar results on four different sperm samples.

showing uniform positivity all over the anterior region of the head, the KIT signal was more heavily concentrated in the equatorial segment (Supplementary Material, Fig. S1).

To ascertain whether KIT positivity in the anterior region of the head was due to co-localization with acrosin within the acrosomal matrix, human spermatozoa were analyzed by laser-scanning confocal immunofluorescence microscopy. As shown in the series of images in Fig. 3B, representing six sequential focal planes of a typical confocal analysis (supplementary Fig. S2B), proceeding from the proximal to the distal plane, the red acrosin signal was the first to appear and the last to disappear with respect to both the green (KIT) equatorial signals and the yellow (KIT-acrosin merge) signal in the anterior region of the head, which were closer to the plane of maximal blue staining (DNA). Thus, KIT positivity appears to be maximal in the sub-acrosomal region of the sperm heads, similar to the perinuclear staining observed in developing spermatids (cfr. Fig. 1B,C).

Molecular identification of TR-KIT as the KIT gene product normally expressed in human spermatozoa

Intracellular KIT immunostaining in the perinuclear region of haploid spermatids and in the sub-acrosomal-equatorial region of sperm heads, suggests that, like in rodents, human post-meiotic KIT positivity might be due to expression of the human equivalent of mouse TR-KIT. In order to clarify this point, we performed western blot analysis of protein extracts from freshly ejaculated human spermatozoa using the same antibody used for the morphological experiments. This antibody is directed against the c-terminal portion shared by both the full-length KIT and TR-KIT. A typical immunoblot analysis is shown in Fig. 4A. No signal was evident in the high molecular weight (MW) range of the blot, indicating that the 150 kDa full-length KIT is not expressed in normal human spermatozoa. However, two lower

Table I Seminal parameters and percentages of positivity (as measured by cytofluorimetric or morphological analysis).

No. of samples	22	23	23	23	23	3	23	23	23	23	23
	% Clusterin (M2) FACS positivity	% Clusterin (M3) FACS positivity	% TUNEL FACS positivity	% TUNEL/ Clusterin (M3) double FACS positivity	% TR-KIT FACS positivity	% TR-KIT FACS positivity after swim-up purification	% Atypical forms (morphological analysis)	Sperm concentration ($n \times 10^6$/ml)	% Forward motility (morphological analysis)	Volume of the ejaculate (ml)	Age (years)
Mean	63.45	28.16	25.03	19.25	52.70	96.37	69.13	115.43	41.74	3.59	41.52
Median	71.65	20.95	18.18	10.93	54.40	95.90	68.00	100.00	45.00	3.80	38.00
Standard deviation	18.88	22.06	20.19	19.14	23.27	1.46	8.26	83.24	14.82	1.52	13.60
Minimum	12.31	7.14	7.71	4.77	10.29	95.20	58.00	25.00	5.00	0.80	22.00
Maximum	86.39	93.43	79.81	68.82	93.30	98.00	88.00	400.00	60.00	6.00	67.00

MW bands, of approximately 50 and 30 kDa were observed. The size of the 30 kDa band coincided exactly with that of a recombinant mouse TR-KIT protein expressed in transfected cell lines. Specificity of these bands was demonstrated by their almost complete disappearance when the primary antibody had been pre-incubated with a 100-fold molar excess (1:1 mass ratio) of the competing immunogenic peptide, whereas other non-specific bands detected in transfected cell lines were not competed. Identical results were obtained in human sperm samples by using the cross-reactive anti-mouse-KIT-c-terminus antibody described by Albanesi *et al.* (1996; data not shown). The specificity of the antibody was confirmed by co-transfecting cell lines with a TR-KIT expressing plasmid and a series of plasmids designed to elicit RNA interference against TR-KIT mRNA (Supplementary Material, Fig. S3).

The 50 and 30 kDa TR-KIT bands were also observed when immunoblot analysis was performed with a human sperm sample in which 100% of spermatozoa lacked the acrosome, confirming that the TR-KIT is not localized inside the acrosomal matrix (Fig. 4B). Immunoblot analysis performed with randomly selected sperm samples from patients recruited for fertility studies, showed that the low MW KIT bands were observed with variable intensity in different subjects, in agreement with the observed variability of KIT immunostaining observed in immunocytochemical, immunofluorescence and cytometric studies in normozoospermic subjects (Fig. 4C). Notably, the relative intensity of the 50 versus the 30 kDa specific bands varied in different samples. Two specific TR-KIT immunoreactive bands of approximately the same MW were observed also in mouse elongating spermatids and in mouse epididymis spermatozoa, and we suggested that the 50 kDa band might be generated by a covalent interaction of the 30 kDa TR-KIT protein with some other protein/s present in haploid cells, but not in transfected cell lines (Albanesi *et al.*, 1996).

Identification of TR-KIT as the *KIT* gene product normally expressed in human spermatozoa was confirmed also at the RNA level through semi-quantitative RT–PCR. Analysis of cDNA obtained from RNA extracted from human spermatozoa of fertile subjects shows that TR-KIT, but not KIT, mRNA is detectable in human sperm (Fig. 4D). Indeed, using as reverse primer an oligonucleotide corresponding to exon 18 (shared by both KIT and TR-KIT) and different forward primers, we observed the positive signal of the expected size (209 bp band) only when the primer annealed to the KIT exon 17 (which corresponds to the first exon of the TR-KIT-specific mRNA expressed during mouse spermiogenesis). By contrast, forward primers that should amplify RNA encoding the full-length KIT receptor (oligonucleotides corresponding to sequences from exon 15 and the beginning of exon 16), did not generate any RT–PCR product even after a higher number of PCR cycles.

Correlation of TR-KIT expression in the sperm heads with sperm DNA integrity

Since lack of the TR-KIT immunostaining was frequently associated with morphological anomalies of the sperm heads, we performed co-staining of KIT and DNA fragmentation, a well-defined marker of sperm head damage, through the TUNEL technique. We also performed co-immunofluorescence staining for KIT and clusterin. Indeed, in bulls, rams and humans, normal spermatozoa are stained by anti-clusterin antibodies, due to the presence of clusterin produced

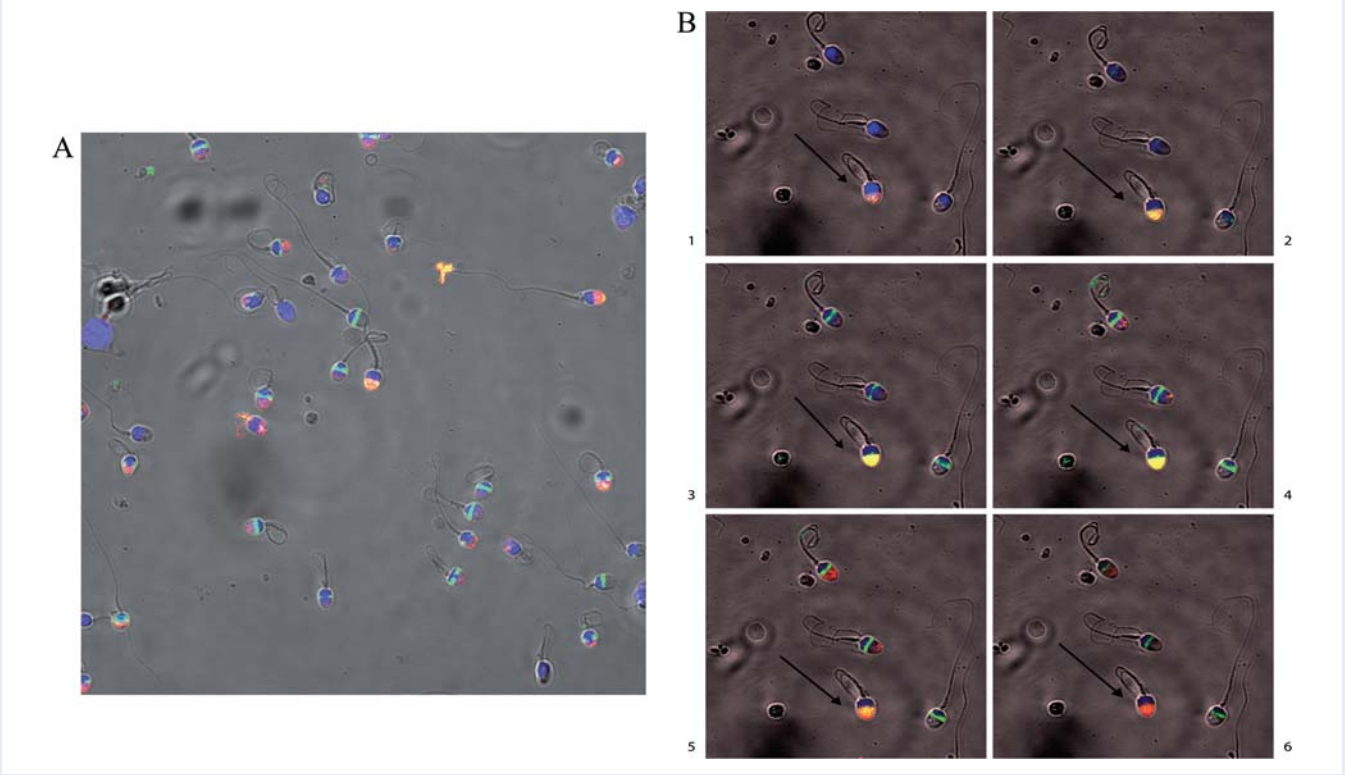

Figure 3 KIT immunostaining in human spermatozoa is mostly confined to the equatorial segment of the sperm heads and sub-acrosomal region. (**A**): representative example of double immunofluorescence analysis for KIT (green signal) and acrosin (red signal) in permeabilized spermatozoa from semen of a normozoospermic donor, using TOTO-3 dye to reveal DNA in sperm heads (blue signal) and transmission microscopy to check sperm morphology. Equatorial localization of KIT signal is evident in most sperm heads, and is present also in spermatozoa which had undergone a spontaneous acrosome reaction (revealed by lack of acrosin staining in the anterior head region). In a minority of cells, KIT and acrosin signals appear to merge in the anterior region of the head (yellow signal). Some sperm cells are KIT-negative but acrosin-positive, and some are negative for both antigens. Most spermatozoa with low or absent KIT reactivity display evident morphological anomalies. (**B**): representative laser-scanning confocal immunofluorescence microscopy images of semen of a normozoospermic donor probed with anti-KIT (green signal) and anti-acrosin (red signal) and counterstained with TOTO-3 dye to reveal DNA in sperm heads (blue signal), overlapped on the background of corresponding transmission microscopy images. Panels from 1 to 6 indicate six sequential focal planes of a typical confocal analysis. An arrow points to a sperm head in which KIT and acrosin signals appeared to merge in the anterior region of the head (yellow-orange signal) in ordinary immunofluorescence observation (supplementary Fig. S2A). In this sperm head, the red (acrosin) signal is mostly evident in the more proximal (1.2) and distal (5.6) planes, whereas the yellow-green (KIT) signals are mostly evident in the central planes (3 and 4).

during the spermatogenic process within the acrosomal cap, whereas morphologically abnormal spermatozoa have an extensive surface coating of a different clusterin isoform all over the sperm length, including the tail, which is not detectable on normal spermatozoa (O'Bryan *et al*., 1994; Ibrahim *et al*., 2000, 2001; Martínez-Heredia *et al*., 2008, Muciaccia *et al*., unpublished data). We routinely observed that most of TR-KIT positive spermatozoa were TUNEL negative or faintly reactive for clusterin in the acrosomal cap, whereas most KIT negative spermatozoa, which often were positive for other sperm head proteins, such as acrosin, were heavily stained by the anti-clusterin antibody and mostly TUNEL positive (Muciaccia *et al*., unpublished data). To quantify these observations, we performed cytometric analysis of 23 sperm samples from volunteer donors, 20 of which were normozoospermic and 3 asthenoteratozoospermic (see Table I for average seminal and cytometric parameters). We observed that TR-KIT positive cells were highly enriched in the TUNEL-negative cell populations (Fig. 5A). Figure 5B shows that the percentage of shift with the anti-KIT antibody in FACS analysis was inversely related to the percentage of M3 shift obtained with the anti-clusterin antibody (corresponding to the abnormal sperm population with a very high immunofluorescence staining due to the extracellular coating of clusterin; Muciaccia *et al*., unpublished data). By contrast, the percentage of shift with the anti-KIT antibody was directly related to the clusterin M2 shift (corresponding to the normal sperm population, which show a moderate immunofluorescence staining due to the intracellular clusterin present in the acrosomal region).

A summary of cytometric data obtained in the 23 sperm samples is shown in Fig. 6A. The lowest levels of TR-KIT expression was found in the semen of two of the three donors, which resulted to be asthenoteratozoospermic. In these samples, we also found the highest levels of DNA damage, as revealed by the TUNEL analysis. Statistical analysis (Table II) revealed a significant (Pearson's coefficient, $r = -0.76$, $P < 0.0001$, $n = 23$) inverse correlation between the percentage of TR-KIT immunolabeling and double positivity for two markers of

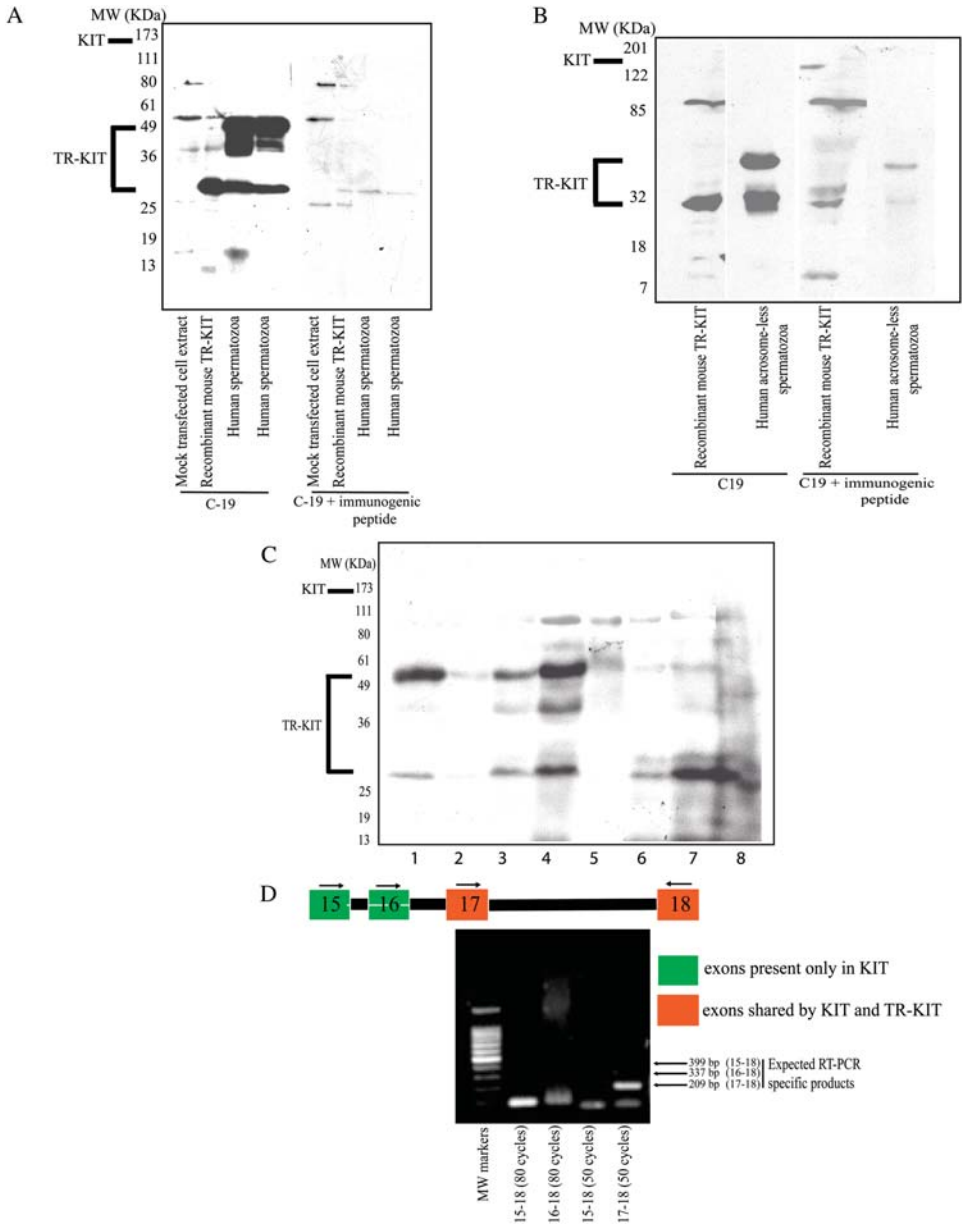

Figure 4 Human spermatozoa express TR-KIT, but not full-length KIT. (**A**): representative immunoblot analysis using the C-19 rabbit polyclonal antibody against the c-terminus of the KIT or the same antibody pre-incubated with an excess of the immunogenic peptides. Protein extracts tested were (left to right) from mock- transfected HEK293 cells, from the same cells transfected with a vector expressing recombinant mouse TR-KIT, and from spermatozoa of two normozoospermic donors. High MW bands corresponding full-length KIT are absent, whereas two specific 50 and 30 kDa TR-KIT bands are evident in both sperm samples. These bands, as well the recombinant 30 kDa TR-KIT band, are almost absent after pre-incubation of C-19 with its cognate epitope. (**B**): immunoblot analysis of protein extracts from semen of a patient in which 100% of spermatozoa lacked the acrosome. The specific TR-KIT bands are evident also in this sample, and high MW bands corresponding full-length KIT are absent. (**C**): immunoblot analysis using the C-19 antibody performed with eight randomly selected sperm samples from patients (indicated by numbers) recruited for fertility studies. The 50 and 30 kDa TR-KIT bands were observed with variable intensity in different subjects and, again, high MW bands corresponding full-length KIT are absent. Equivalent protein loading was checked by reversible Ponceau staining before probing blots with the C-19 antibody. (**D**): a representative RT–PCR analysis of RNA extracted from spermatozoa of a normozoospermic donor, indicates that RNA encoding for TR-KIT, but not for full-length KIT, is detectable in human spermatozoa as a remnant of transcription occurring during spermiogenesis. The low MW bands present on the bottom of the lanes are due to the oligonucleotide primers used for amplification. No signals were obtained when omitting RT before the amplification step of the reaction. This experiment was repeated on RNA extracted from sperm samples from three different normozoospermic donors with similar results.

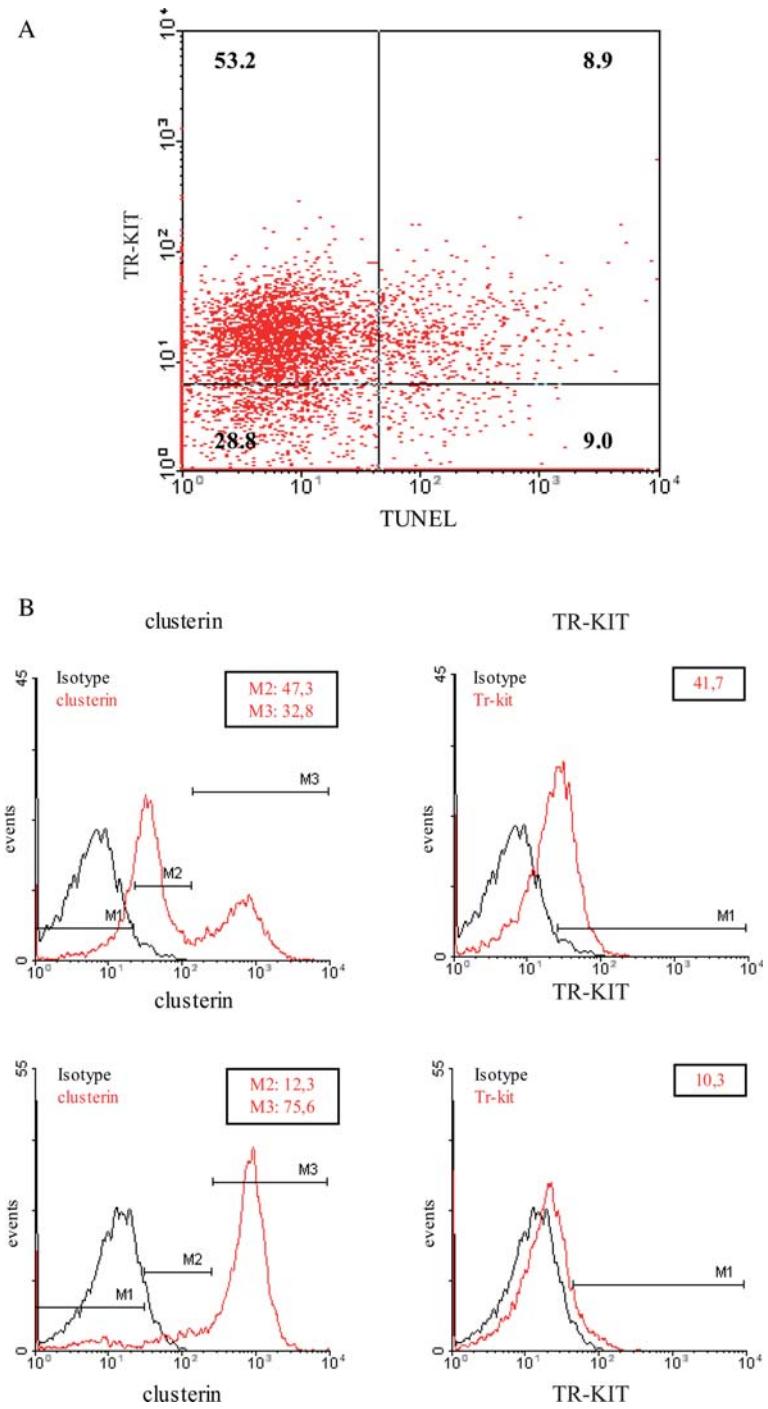

Figure 5 TR-KIT expressing spermatozoa have a low level of DNA damage and an high percentage of TR-KIT positivity corresponds to low levels of staining with anti-clusterin antibodies. (**A**): representative double cytometric analysis for TR-KIT immuno-positivity and DNA fragmentation.on a sperm sample from a normozoospermic donor. Permeabilized spermatozoa were treated by *In Situ* Cell Death Detection Kit-Fluorescein (Roche, Italy) before TR-KIT immunolabeling. with the C-19 antibody. Numbers within different gate quadrants refer to the percentage of: TR-KIT positive/TUNEL negative (top left), TR-KIT negative/TUNEL negative (bottom left); TR-KIT positive/TUNEL positive (top right), and TR-KIT negative/TUNEL positive cells (bottom right). TR-KIT positive cells appear to be highly enriched in the TUNEL-negative cell population. (**B**): representative contemporary cytometric analysis with anti-clusterin (left panels) and anti-KIT (right panels) antibodies of permeabilized sperm samples from two different donors, showing either high (top panels) or low (bottom panels) percentage of TR-KIT positivity (M1 peaks). In the sperm sample with high TR-KIT positivity (top panels), two separate peaks of clusterin positivity (M2 and M3) are evident: the M2 clusterin peak corresponds to spermatozoa with moderate anti-clusterin staining in the acrosomal cap, whereas the M3 peak corresponds to spermatozoa with intense surface anti-clusterin staining (Muciaccia *et al.*, unpublished data). In the sperm sample with low percentage of TR-KIT positivity (bottom panels), only the clusterin M3 peak is evident.

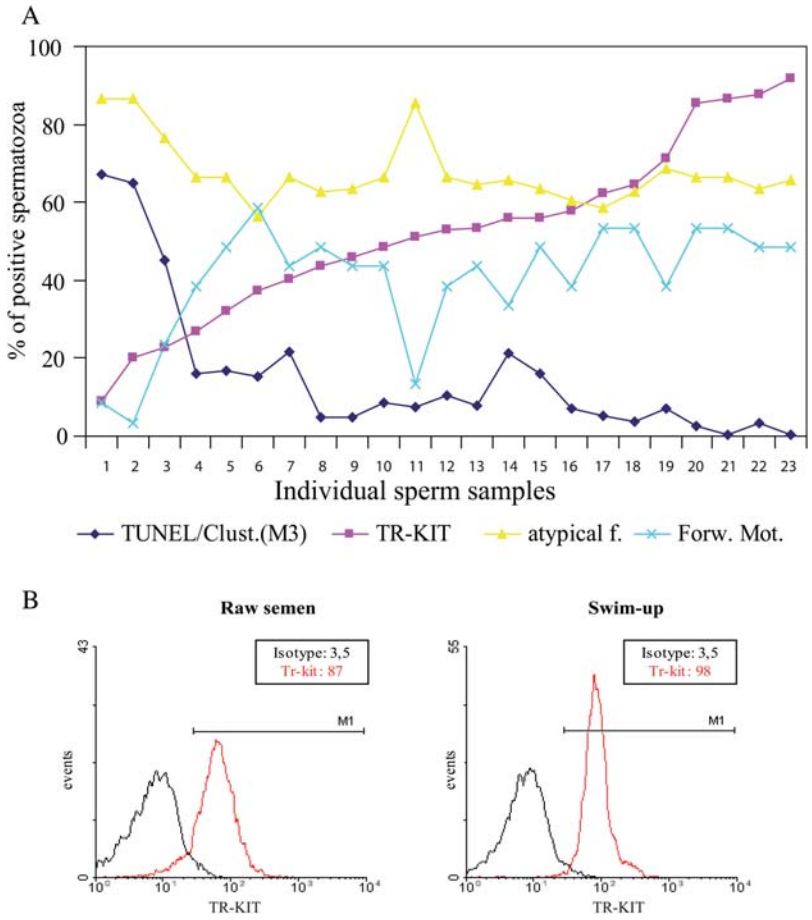

Figure 6 Correlation of TR-KIT presence in human sperm heads with semen quality. (**A**): graphic summary of cytometric data observed in sperm samples from 23 volunteer donors. Individual sperm samples shown on the *X*-axis were ordered according to increasing percentages of TR-KIT immunolabeling. In the same graph, we plotted the percentages values of cytometric double positivity for both TUNEL and intense clusterin immunolabeling (M3 peak); percentage of morphologically observed sperm atypical forms; percentages of forward (rectilinear) sperm motility. The inverse correlation between TR-KIT positivity and positivity for markers of sperm damage, i.e. double positivity for TUNEL and clusterin.(M3), is clear, whereas inverse correlation with the levels of atypical forms and direct correlation with forward motility are less evident. (**B**): representative example of quantification of the percentage of KIT immunolabeling in permeabilized human spermatozoa from a normozoospermic donor using flow cytometry with the C-19 antibody, before (left panel) and after (right panel) swim-up purification of the semen sample.

sperm damage, i.e. TUNEL positivity and intense clusterin immunolabeling (M3 peak). Conversely, these two negative parameters appeared to be in strong direct correlation to each other ($r = 0.96$, $P < 0.00001$, $n = 23$). In the semen samples from the same subjects, we also found a less significant direct correlation between TR-KIT positivity and sperm forward motility parameters ($r = 0.59$, $P < 0.01$, $n = 23$), and inverse correlation to the microscopically observed percentage of sperm head atypical forms ($r = -0.47$, $P < 0.05$, $n = 23$). A significant inverse correlation was also found between percentages of TR-KIT immunolabeling with increasing donors' age ($r = -0.73$, $P < 0.0001$, $n = 23$), whereas no correlation was found between TR-KIT positivity and other semen parameters, such as sperm concentration ($r = 0.00$) or volume of the ejaculate ($r = -0.05$).

The most interesting data emerging from the FACS analysis is that the average percentage of TUNEL positivity in unselected sperm samples was 25.03 $\pm$ 20.19 (median value: 18.18; $n = 23$; Table I), whereas double positivity for both TUNEL and TR-KIT dropped to 7.69 $\pm$ 5.12 (median value: 6.81; $n = 17$). Thus, percentages of TR-KIT immunolabeling of human spermatozoa correlates to sperm DNA integrity, suggesting that it might constitute a positive marker of semen quality in human fertility studies. Further support to this hypothesis was obtained by comparing cytometric analysis of three total unselected sperm samples with that of the same samples after swim-up purification (see a representative example in Fig. 6B). An enrichment of TR-KIT immunolabeling was constantly observed after swim-up selections in all sperm samples tested, demonstrating that motile spermatozoa are an homogeneous population of TR-KIT immunoreactive cells (percentage of TR-KIT positivity in the three semen samples: 88.03 $\pm$ 0.85 in the raw semen, and 96.37 $\pm$ 1.18 after swim-up selection).

Discussion

Infertile men are often characterized by a reduced sperm number, impaired sperm morphology, low sperm motility or, in many cases,

Table II Analysis of statistical correlation between seminal parameters and cytofluorimetric data (*r*-values = Pearson's product-moment correlation coefficients)

	% Clusterin (M3)	% TUNEL	% TUNEL/Clusterin (M3) Double positivity	% TR-KIT	% Atypical forms	Sperm concentration	% Forward motility	Volume of the ejaculate	Age
% Clusterin (M2)	−0.944	−0.898	−0.896	0.714	−0.604	−0.146	0.682	0.197	−0.819
% Clusterin (M3)		0.964	0.958	−0.719	0.784	−0.074	−0.851	−0.038	0.731
%TUNEL			0.981	−0.715	0.797	−0.085	−0.839	−0.126	0.742
% TUNEL+Clusterin (M3) double positivity				−0.763	0.729	−0.085	−0.786	−0.076	0.696
% TR-KIT					−0.469	0.007	0.590	−0.056	−0.733
% Atypical forms						−0.360	−0.921	−0.062	0.625
Sperm concentration							0.388	−0.576	0.114
% Forward motility								−0.018	−0.640
Volume of the ejaculate									−0.267

by a combination of all these factors. A less frequent cause of unexplained male infertility is failure in egg activation after sperm–oocyte fusion and/or block in the early embryonic development. The non-genomic paternal contribution to egg activation consists of triggering meiotic resumption of the oocytes from their block in metaphase II (Barroso *et al*., 2009). Mouse TR-KIT is one of the candidate sperm factors acting in egg activation at fertilization (Sette *et al*., 1997, 1998, 2002; Paronetto *et al*., 2003).

In this paper, we show that TR-KIT protein is expressed during human spermiogenesis and maintained in human spermatozoa, suggesting a conserved functional role for this alternative product of the *KIT* gene during male gametogenesis and/or at fertilization. In contrast with previous claims (Feng *et al*., 2005), in human spermatozoa, we found no trace of full-length KIT. This was confirmed by our finding that RNA encoding for TR-KIT, but not for full-length KIT, is present in human spermatozoa, likely as a remnant of transcription occurring during human spermiogenesis (Miller *et al*., 1994).

Besides TR-KIT, other candidate sperm factors for egg activation are phospholipase C zeta (PLCZETA) (Saunders *et al*., 2002) and post-acrosomal sheath WW domain-binding protein (PAWP) (Wu *et al*., 2007a). PLCZETA was shown to induce oocyte activation from the mouse sperm perinuclear matrix. (Fujimoto *et al*., 2004). Moreover, PLCZETA is localized in the equatorial segment of bull sperm (Yoon and Fissore, 2007), and in the acrosomal, equatorial and post-acrosomal segments of human sperm (Grasa *et al*., 2008). PAWP exclusively resides in the post-acrosomal sheath of guinea pig and bull sperm (Wu *et al*., 2007a, b). Sperm deficient in oocyte activation have been shown to lack equatorial localization of PLCZETA, and immunoblot analysis showed reduced amounts of PLCZETA in sperm from infertile men (Yoon *et al*., 2008; Heytens *et al*., 2009). However, it cannot be excluded that other factors present in the perinuclear theca (PT) and/or in the equatorial region might equally be absent in spermatozoa that are unable to trigger egg activation.

PT (the cytoskeletal coat of the mammalian sperm nucleus that is removed from the sperm head at fertilization) plays a role in joining the acrosome and the post-acrosomal plasma membrane to the nucleus during spermiogenesis. In addition, it has been proposed that PT might harbor the sperm borne oocyte-activating factors (SOAFs), which trigger the signaling cascade of oocyte activation (Kimura *et al*., 1998; Sutovsky and Schatten, 2000; Ito *et al*., 2009).

The appearance and localization of the sub-acrosomal PT during human spermiogenesis is tightly associated with acrosomal biogenesis (Alvarez Sedó *et al*., 2009). We found that, during human spermiogenesis, the TR-KIT is strongly concentrated in the perinuclear region of spermatids and in the area of the developing acrosome. In mature spermatozoa the TR-KIT is present in the sub-acrosomal layer of the human sperm head, where the PT is found, and it is highly concentrated in the equatorial segment, similarly to PLCZETA.

Since the equatorial segment and the post-acrosomal regions are the first part of the head which fuses with the egg membrane (Florman and Ducibella, 2006), localization of all the three main candidate SOAFs (TR-KIT, PLCZETA, PAWP) seems to be consistent with a possible function in egg activation. However, due to the lack of knock-out mice genetic models, the precise physiological role of TR-KIT, as well as that of other candidate SOAFs, in triggering early embryogenesis remains unknown. It is also possible (and likely) that

more than a single sperm factor is actually required for full egg activation and progression of early embryonic development.

Regardless of the physiological role played by TR-KIT, however, another important result of our present study is the direct correlation between its presence in human sperm heads and sperm DNA integrity.

TR-KIT expressing spermatozoa were highly enriched in the TUNEL- and clusterin-negative sperm cell populations, whereas spermatozoa with evident morphological anomalies were frequently TR-KIT negative. The percentage of spermatozoa carrying TR-KIT showed a broad variation between different sperm samples from unselected volunteer donors. However, almost 100% of the TR-KIT positivity was evident in sperm samples after swim-up selection.

The coincidence of TR-KIT absence and both DNA fragmentation and the high clusterin-positivity, does not appear as a mere consequence of general loss of other proteins in damaged or malformed spermatozoa, since these often retain an intact acrosome in the anterior region of the head, as revealed by the positive staining for acrosin. TR-KIT localization in the perinuclear region of the sperm head might imply an altered formation or damage of the PT as the basis for the correlation between TR-KIT negativity and DNA fragmentation.

Since the TR-KIT expression appears to correlate particularly with sperm DNA integrity, we propose that TR-KIT could be a new marker for evaluating human semen quality, particularly in sperm samples from subjects enrolled in ARTs such as *in vitro* fertilization (IVF) or ICSI.

Several reports showed no significant correlation between sperm DNA damage and fertilization rates after ICSI (Bungum *et al*., 2004; Gandini *et al*., 2004; Greco *et al*., 2005; Li *et al*., 2006; Bakos *et al*., 2008), whereas other reports have shown a negative correlation (Lopes *et al*., 1998; Benchaib *et al*., 2003; Huang *et al*., 2005). These apparent discrepancies could be explained by the technical nature of ICSI, in which morphologically normal sperm cells are selected for injection, thus increasing the chance of using a sperm with intact DNA, by the nature and extent of the DNA damage, and by the variation in DNA repair ability of microinjected oocytes.

Sperm DNA damage might cause arrest of embryonic development at stages in which expression of the paternal genome is required, however impairment of fertilization has been observed even at the level of pronuclei formation (reviewed by Barroso *et al*., 2009). Since the first steps of embryonic development are mostly under the control of maternal transcripts, these studies suggest that sperm cells carrying DNA damage might also have a lower intrinsic fertilizing capacity.

Our finding that the TR-KIT, a candidate SOAF is absent, or present at lower levels, in DNA damaged spermatozoa, might contribute, at least in part, to their low efficiency in triggering fertilization and/or normal embryonic development after IVF or ICSI reported in some studies.

In conclusion, we have shown that the TR-KIT is present in human ejaculated spermatozoa, where it is localized in the sub-acrosomal and equatorial segment. The equatorial localization of TR-KIT is compatible with its proposed function as a sperm factor at fertilization. Moreover, we found a significant inverse correlation of TR-KIT positivity with markers of sperm DNA damage. Thus, evaluation of the TR-KIT expression by cytometric analysis might be a predictive parameter of human semen quality, which could be analyzed in hypofertile or infertile subjects. Since we show that high levels of clusterin immunolabeling strongly correlate with DNA fragmentation, our data also suggest that FACS selection with anti-clusterin antibodies of unpermeabilized sperm cells might be used to remove spermatozoa with high levels of DNA damage and low expression of TR-KIT (and, eventually, of other candidate SOAFs which co-localize in the PT).

Funding

Work was supported by PRIN 2007 grant to P.R. and M.S. (project 200788TPYE_002), and by grants MFAG 4765 (AIRC) and "Rientro dei Cervelli" (MIUR) to M.B.

Acknowledgements

We thank Jan Tesarik (Center for Reproductive Medicine, European Hospital, Rome, Italy) and Giovanni Bertalot (Ospedale di Leno, Brescia, Italy) for the gift of human specimens, Annarita Di Sauro for help in recombinant DNA studies (RNA interference in transfected cell lines), Fabrizio Padula and Stefania De Grossi for technical supports in cytometric analysis and confocal microscopy, respectively.

Supplementary data

Supplementary data are available at http://humrep.oxfordjournals.org/.

References

Agarwal A, Said TM. Role of sperm chromatin abnormalities and DNA damage in male infertility. *Hum Reprod Update* 2003;**9**:331–345.

Agarwal A, Makker K, Sharma R. Clinical relevance of oxidative stress in male factor infertility: an update. *Am J Reprod Immunol* 2008;**59**:2–11.

Aitken RJ, De Iuliis GN, McLachlan RI. Biological and clinical significance of DNA damage in the male germ line. *Int J Androl* 2009;**32**:46–56.

Albanesi C, Geremia R, Giorgio M, Dolci S, Sette C, Rossi P. A cell- and developmental stage-specific promoter drives the expression of a truncated c-kit protein during mouse spermatid elongation. *Development* 1996;**122**:1291–1302.

Alvarez Sedó C, Oko R, Sutovsky P, Chemes H, Rawe VY. Biogenesis of the sperm head perinuclear theca during human spermiogenesis. *Fertil Steril* 2009;**92**:1472–1473.

Bakos HW, Thompson JG, Feil D, Lane M. Sperm DNA damage is associated with assisted reproductive technology pregnancy. *Int J Androl* 2008;**31**:518–526.

Barratt CL, Aitken RJ, Björndahl L, Carrell DT, de Boer P, Kvist U, Lewis SE, Perreault SD, Perry MJ, Ramos L *et al*. Sperm DNA: organization, protection and vulnerability: from basic science to clinical applications–a position report. *Hum Reprod* 2010; Feb 6. [Epub ahead of print].

Barroso G, Valdespin C, Vega E, Kershenovich R, Avila R, Avendaño C, Oehninger S. Developmental sperm contributions: fertilization and beyond. *Fertil Steril* 2009;**92**:835–848.

Benchaib M, Braun V, Lornage J, Hadj S, Salle B, Lejeune H, Guérin JF. Sperm DNA fragmentation decreases the pregnancy rate in an assisted reproductive technique. *Hum Reprod* 2003;**18**:1023–1028.

Bungum M, Humaidan P, Spano M, Jepson K, Bungum L, Giwercman A. The predictive value of sperm chromatin structure assay (SCSA)

parameters for the outcome of intrauterine insemination, IVF and ICSI. *Hum Reprod* 2004;**19**:1401–1408.

Feng HL, Sandlow JI, Zheng LJ. C-kit receptor and its possible function in human spermatozoa. *Mol Reprod Dev* 2005;**70**:103–110.

Florman HM, Ducibella T. Fertilization in mammals. In: Neill JD (ed). *Knobil and Neill's Physiology of Reproduction*, 3rd edn. St. Louis, MO: Elsevier Academic Press, 2006, 55–112.

Fujimoto S, Yoshida N, Fukui T, Amanai M, Isobe T, Itagaki C, Izumi T, Perry AC. Mammalian phospholipase Czeta induces oocyte activation from the sperm perinuclear matrix. *Dev Biol* 2004;**274**:370–383.

Gandini L, Lombardo F, Paoli D, Caruso F, Eleuteri P, Leter G, Ciriminna R, Culasso F, Dondero F, Lenzi A *et al.* Full-term pregnancies achieved with ICSI despite high levels of sperm chromatin damage. *Hum Reprod* 2004;**19**:1409–1417.

Grasa P, Coward K, Young C, Parrington J. The pattern of localization of the putative oocyte activation factor, phospholipase Czeta, in uncapacitated, capacitated, and ionophore-treated human spermatozoa. *Hum Reprod* 2008;**23**:2513–2522.

Greco E, Romano S, Iacobelli M, Ferrero S, Baroni E, Minasi MG, Ubaldi F, Rienzi L, Tesarik J. ICSI in cases of sperm DNA damage: beneficial effect of oral antioxidant treatment. *Hum Reprod* 2005;**20**:2590–2594.

He Z, Kokkinaki M, Jiang J, Dobrinski I, Dym M. Isolation, characterization, and culture of human spermatogonia. *Biol Reprod* 2010;**82**:363–372.

Heytens E, Parrington J, Coward K, Young C, Lambrecht S, Yoon SY, Fissore RA, Hamer R, Deane CM, Ruas M *et al.* Reduced amounts and abnormal forms of phospholipase C zeta (PLCzeta) in spermatozoa from infertile men. *Hum Reprod* 2009;**24**:2417–2428.

Huang CC, Lin DP, Tsao HM, Cheng TC, Liu CH, Lee MS. Sperm DNA fragmentation negatively correlates with velocity and fertilization rates but might not affect pregnancy rates. *Fertil Steril* 2005;**84**:130–140.

Ibrahim NM, Gilbert GR, Loseth KJ, Crabo BG. Correlation between clusterin-positive spermatozoa determined by flow cytometry in bull semen and fertility. *J Androl* 2000;**21**:887–894.

Ibrahim NM, Romano JE, Troedsson MH, Crabo BG. Effect of scrotal insulation on clusterin-positive cells in ram semen and their relationship to semen quality. *J Androl* 2001;**22**:863–877.

Irvine DS, Twigg JP, Gordon EL, Fulton N, Milne PA, Aitken RJ. DNA integrity in human spermatozoa: relationships with semen quality. *J Androl* 2000;**21**:33–44.

Ito C, Akutsu H, Yao R, Kyono K, Suzuki-Toyota F, Toyama Y, Maekawa M, Noda T, Toshimori K. Oocyte activation ability correlates with head flatness and presence of perinuclear theca substance in human and mouse sperm. *Hum Reprod* 2009; **24**:2588–2595.

Kimura Y, Yanagimachi R, Kuretake S, Bortkiewicz H, Perry AC, Yanagimachi H. Analysis of mouse oocyte activation suggests the involvement of sperm perinuclear material. *Biol Reprod* 1998; **58**:1407–1415.

Levi M, Shalgi R. The role of Fyn kinase in the release from metaphase in mammalian oocytes. *Mol Cell Endocrinol* 2010;**314**:228–233.

Lewis SE. Importance of mitochondrial and nuclear sperm DNA in sperm quality assessment and assisted reproduction outcome. *Hum Fertil (Camb)* 2002;**5**:102–109.

Li Z, Wang L, Cai J, Huang H. Correlation of sperm DNA damage with IVF and ICSI outcomes: a systematic review and meta-analysis. *J Assist Reprod Genet* 2006;**23**:367–376.

Lopes S, Sun JG, Jurisicova A, Meriano J, Casper RF. Sperm deoxyribonucleic acid fragmentation is increased in poor-quality semen samples and correlates with failed fertilization in intracytoplasmic sperm injection. *Fertil Steril* 1998;**69**:528–532.

Luo J, McGinnis LK, Kinsey WH. Fyn kinase activity is required for normal organization and functional polarity of the mouse oocyte cortex. *Mol Reprod Dev* 2009;**76**:819–831.

Martínez-Heredia J, de Mateo S, Vidal-Taboada JM, Ballescà JL, Oliva R. Identification of proteomic differences in asthenozoospermic sperm samples. *Hum Reprod* 2008;**23**:783–791.

McGinnis LK, Albertini DF, Kinsey WH. Localized activation of Src-family protein kinases in the mouse egg. *Dev Biol* 2007;**306**:241–254.

Meng L, Luo J, Li C, Kinsey WH. Role of Src homology 2 domain-mediated PTK signaling in mouse zygotic development. *Reproduction* 2006; **132**:413–421.

Miller D, Tang PZ, Skinner C, Lilford R. Differential RNA fingerprinting as a tool in the analysis of spermatozoal gene expression. *Hum Reprod* 1994; **9**:864–869.

Muciaccia B, Corallini S, Vicini E, Padula F, Gandini L, Liuzzi G, Lenzi A, Stefanini M. HIV-1 viral DNA is present in ejaculated abnormal spermatozoa of seropositive subjects. *Hum Reprod* 2007; **22**:2868–2878.

Natali PG, Nicotra MR, Sures I, Santoro E, Bigotti A, Ullrich A. Expression of c-kit receptor in normal and transformed human non-lymphoid tissues. *Cancer Res* 1992;**52**:6139–6143.

O'Bryan MK, Murphy BF, Liu DY, Clarke GN, Baker HW. The use of anticlusterin monoclonal antibodies for the combined assessment of human sperm morphology and acrosome integrity. *Hum Reprod* 1994; **9**:1490–1496.

Paronetto MP, Venables JP, Elliott DJ, Geremia R, Rossi P, Sette C. TR-KIT promotes the formation of a multimolecular complex composed by Fyn, PLCγ1 and Sam68. *Oncogene* 2003;**22**:8707–8715.

Paronetto MP, Farini D, Sammarco I, Maturo G, Vespasiani G, Geremia R, Rossi P, Sette C. Expression of a truncated form of the c-kit tyrosine kinase receptor and activation of Src kinase in human prostatic cancer. *Am J Pathol* 2004;**164**:1243–1251.

Pellegrini M, Filipponi D, Gori M, Barrios F, Lolicato F, Grimaldi P, Rossi P, Jannini EA, Geremia R, Dolci S. ATRA and KL promote differentiation toward the meiotic program of male germ cells. *Cell Cycle* 2008; **7**:3878–3888.

Prabhu SM, Meistrich ML, McLaughlin EA, Roman SD, Warne S, Mendis S, Itman C, Loveland KL. Expression of c-Kit receptor mRNA and protein in the developing, adult and irradiated rodent testis. *Reproduction* 2006; **131**:489–499.

Reut TM, Mattan L, Dafna T, Ruth KK, Ruth S. The role of Src family kinases in egg activation. *Dev Biol* 2007;**312**:77–89.

Rossi P, Marziali G, Albanesi C, Charlesworth A, Geremia R, Sorrentino V. A novel c-kit transcript, potentially encoding a truncated receptor, originates within a kit gene intron in mouse spermatids. *Dev Biol* 1992;**152**:203–207.

Rossi P, Sette C, Dolci S, Geremia R. Role of c-kit in mammalian spermatogenesis. *J Endocrinol Invest* 2000;**23**:609–615.

Rossi P, Dolci S, Sette C, Geremia R. Molecular mechanisms utilized by alternative c-kit gene products in the control of spermatogonial proliferation and sperm-mediated egg activation. *Andrologia* 2003; **35**:71–78.

Sakamoto A, Yoneda A, Terada K, Namiki Y, Suzuki K, Mori T, Ueda J, Watanabe T. A functional truncated form of c-kit tyrosine kinase is produced specifically in the testis of the mouse but not the rat, pig, or human. *Biochem Genet* 2004;**42**:441–451.

Saleh RA, Agarwal A, Nelson DR, Nada EA, El-Tonsy MH, Alvarez JG, Thomas AJ Jr, Sharma RK. Increased sperm nuclear DNA damage in normozoospermic infertile men: a prospective study. *Fertil Steril* 2002; **78**:313–318.

Sandlow JI, Feng HL, Cohen MB, Sandra A. Expression of c-KIT and its ligand, stem cell factor, in normal and subfertile human testicular tissue. *J. Androl* 1996;**17**:403–408.

Saunders CM, Larman MG, Parrington J, Cox LJ, Royse J, Blayney LM, Swann K, Lai FA. PLC zeta: a sperm-specific trigger of $Ca(2^+)$ oscillations in eggs and embryo development. *Development* 2002; **129**:3533–3544.

Sette C, Bevilacqua A, Bianchini A, Mangia F, Geremia R, Rossi P. Parthenogenetic activation of mouse eggs by microinjection of a truncated c-kit tyrosine kinase present in spermatozoa. *Development* 1997;**124**:2267–2274.

Sette C, Bevilacqua A, Geremia R, Rossi P. Involvement of phospholipase C γ1 in mouse egg activation induced by a truncated form of the c-kit tyrosine kinase present in spermatozoa. *J Cell Biol* 1998; **142**:1063–1074.

Sette C, Dolci S, Geremia R, Rossi P. Role of stem cell factor and of alternative c-kit gene products in the establishment, maintenance and function of the germ cells. *Int J Dev Biol* 2000;**44**:599–608.

Sette C, Paronetto MP, Barchi M, Bevilacqua A, Geremia R, Rossi P. TR-KIT-induced resumption of the cell cycle in mouse eggs requires activation of a Src-like kinase. *EMBO J* 2002;**21**:5386–5395.

Shinagawa T, Ishii S. Generation of Ski-knockdown mice by expressing a long double-strand RNA from an RNA polymerase II promoter. *Genes Dev* 2003;**17**:1340–1345.

Sorrentino V, Giorgi M, Geremia R, Besmer P, Rossi P. Expression of the *c-kit* protooncogene in the murine male germ cells. *Oncogene* 1991; **6**:149–151.

Strohmeyer T, Reese D, Press M, Ackermann R, Hartmann M, Slamon D. Expression of the c-kit proto-oncogene and its ligand stem cell factor (SCF) in normal and malignant human testicular tissue. *J Urol* 1995; **153**:511–515.

Sutovsky P, Schatten G. Paternal contributions to the mammalian zygote: fertilization after sperm-egg fusion. *Int Rev Cytol* 2000;**195**:1–65.

Takaoka A, Toyota M, Hinoda Y, Itoh F, Mita H, Kakiuchi H, Adachi M, Imai K. Expression and identification of aberrant c-kit transcripts in human cancer cells. *Cancer Lett* 1997;**115**:257–261.

Tomashov-Matar R, Levi M, Shalgi R. The involvement of Src family kinases (SFKs) in the events leading to resumption of meiosis. *Mol Cell Endocrinol* 2008;**282**:56–62.

Toyota M, Hinoda Y, Itoh F, Takaoka A, Imai K, Yachi A. Complementary DNA cloning of truncated form of c-kit in human colon carcinoma cells. *Cancer Res* 1994;**54**:272–275.

Unni SK, Modi DN, Pathak SG, Dhabalia JV, Bhartiya D. Stage-specific localization and expression of c-kit in the adult human testis. *J Histochem Cytochem* 2009;**57**:861–869.

von Schonfeldt V, Krishnamurthy H, Foppiani L, Schlatt S. Magnetic cell sorting is a fast and effective method of enriching viable spermatogonia from Djungarian hamster, mouse, and marmoset monkey testes. *Biol Reprod* 1999;**61**:582–589.

World Health Organization. WHO laboratory manual for the examination of human semen and sperm-cervical mucus interaction. 4th edn, Cambridge, UK: Cambridge University Press, 1999.

Wu AT, Sutovsky P, Manandhar G, Xu W, Katayama M, Day BN, Park KW, Yi YJ, Xi YW, Prather RS *et al.* PAWP, a sperm-specific WW domain-binding protein, promotes meiotic resumption and pronuclear development during fertilization. *J Biol Chem* 2007a; **282**:12164–12175.

Wu AT, Sutovsky P, Xu W, van der Spoel AC, Platt FM, Oko R. The post-acrosomal assembly of sperm head protein, PAWP, is independent of acrosome formation and dependent on microtubular manchette transport. *Dev Biol* 2007b;**312**:471–483.

Yoon SY, Fissore RA. Release of phospholipase C zeta and [Ca2 +]i oscillation-inducing activity during mammalian fertilization. *Reproduction* 2007;**134**:695–704.

Yoon SY, Jellerette T, Salicioni AM, Lee HC, Yoo MS, Coward K, Parrington J, Grow D, Cibelli JB, Visconti PE *et al.* Human sperm devoid of PLC, zeta 1 fail to induce $Ca(2^+)$ release and are unable to initiate the first step of embryo development. *J Clin Invest* 2008;**118**:3671–3681.

Zayas J, Spassov DS, Nachtman RG, Jurecic R. Murine hematopoietic stem cells and multipotent progenitors express truncated intracellular form of c-kit receptor. *Stem Cells Dev* 2008;**17**: 343–353.